Title

Optical Characterization of a Bimorph Deformable Mirror

ISBN

9780791842249

Authors

Horsley, David A

Park, Hyunkyu

Chuang, Chih-Wei

et al.

Publication Date

2005

DOI

10.1115/imece2005-81836

Peer reviewed

Proceedings of IMECE2005
2005 ASME International Mechanical Engineering Congress and Exposition
November 5-11, 2005, Orlando, Florida USA

IMECE2005-81836

OPTICAL CHARACTERIZATION OF A BIMORPH DEFORMABLE MIRROR

David A. Horsley
Department of Mechanical and Aeronautical Engineering
University of California, Davis

Hyunkyu Park
Department of Mechanical and Aeronautical Engineering
University of California, Davis

Chih-Wei Chuang
Department of Mechanical and Aeronautical Engineering
University of California, Davis

Sophie P. Laut
Department of Ophthalmology and Vision Science
University of California, Davis

John S. Werner
Department of Ophthalmology and Vision Science
University of California, Davis

ABSTRACT

This paper reports the results of interferometric characterization of a bimorph deformable mirror (DM) designed for use in an adaptive optics (AO) system. The natural frequencies of this DM were measured up to 20 kHz using both a custom stroboscopic phase-shifting interferometer as well as a commercial Laser Doppler Vibrometer (LDV). Interferometric measurements of the DM surface profile were analyzed by fitting the surface with mode-shapes predicted using classical plate theory for an elastically-supported disk. The measured natural frequencies were found to be in good agreement with the predictions of the theoretical model.

INTRODUCTION

Originally developed to remove atmospheric distortion from astronomical imaging systems, adaptive optics (AO) has seen more recent application to ophthalmologic instruments and free-space optical communication systems. In each of these applications, the AO system uses a deformable mirror (DM) to correct for optical aberrations by removing phase distortions from the incident wavefront. Since the existing DM technology developed for astronomy is expensive and bulky, recent research has focused on using MEMS technology to create a more compact, low-cost DM. Several MEMS DM designs have been demonstrated, including: membrane-based (OKO Technologies Inc.) [1]; polysilicon surface-micromachined (Boston Micromachines Inc.) [2]; bulk silicon (Iris AO Inc.) [3]; and piezoelectric monomorphs (JPL) [4]. Many MEMS DM designs have been driven by the motivation to produce DMs with hundreds or thousands of actuators. For applications which require the correction of only low-order aberrations (such as defocus, astigmatism, coma, and spherical aberration), a DM with less than 100 actuators may be the best choice, as such a device can be lower in cost and complexity than a DM with higher actuator count.

We have chosen to investigate the characteristics of a bimorph MEMS DM manufactured by AOptix Inc. We have tested a total of three DM units from AOptix, each having similar characteristics with the exception of small manufacturing differences. We described an open-loop method for characterizing the static deformation characteristics of this DM in an earlier publication [5], and demonstrated the ability of this DM to reproduce aberrations described by the Zernike polynomials up to the 5^{th} order. Dalimier and Dainty [6] recently compared this DM and two others, demonstrating the ability of the three DMs to correct for the aberrations found in a typical human eye. In this paper, we report on the dynamic characteristics of the DM in response to transient inputs. These dynamic characteristics are important in closed-loop AO systems which require bandwidths close to the first resonance frequency of the DM.

DESCRIPTION OF THE DEFORMABLE MIRROR

The layout of the AOptix DM is illustrated in plan view and cross-section in Figure 1. The device is composed of two 160 μm thick layers of the electrostrictive ceramic lead magnesium niobate (PMN). Metal electrodes are deposited onto the PMN and the two layers are bonded together with a 25 μm thick layer of conductive adhesive. The metallization on the back face of the DM is patterned to produce 36 electrodes, while the uniform metallization on the front face of the DM produces a single front face electrode. The DM is 20 mm in diameter, with only the center 10.2 mm of the DM used as an optical surface in order to reduce the effect of the edge supports on the DM surface profile.

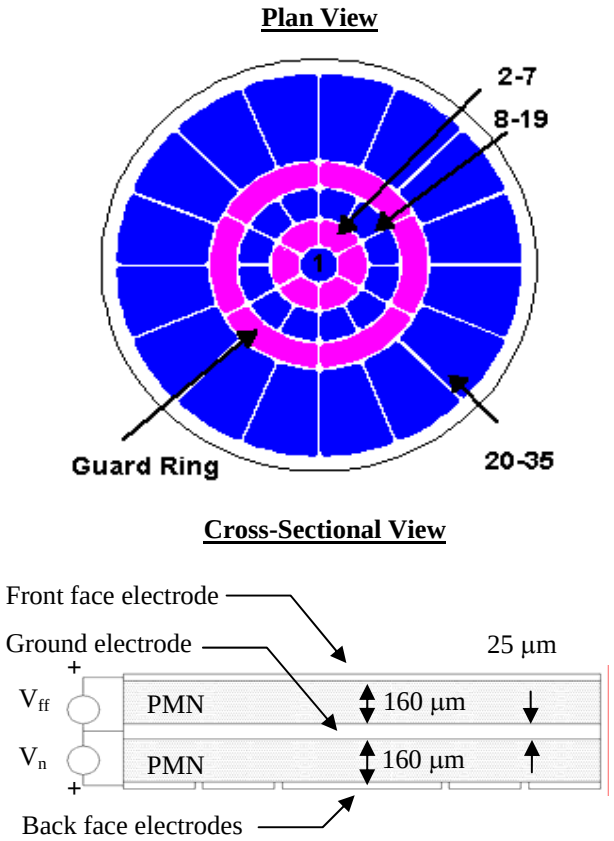

Figure 1: Layout of the AOptix DM: plan view of electrodes (top) and cross-sectional view (bottom). The numbering of the actuator channels is indicated on the plan view.

As illustrated in the figure, voltage is applied to the electrodes on the front and back faces of the DM, with the inner bonded electrodes serving as ground contacts for both layers. The electrodes on the back face of the DM consist of a central pad surrounded by four annular rings of electrodes. The central pad and the electrodes in the two inner rings (channels 1-19) are used to generate local curvature in the mirror surface, while the electrodes in the outer ring (channels 20-35) produce a slope at the edge of the DM. The curvature and slope electrodes are separated by the third annular electrode ring which defines the 10 mm pupil. The completed mirror assembly is mounted in a housing with manual tip-tilt adjustment and a 10.2 mm clear aperture. Residual stress from the manufacturing process results in a slight parabolic curvature to the DM surface when all the electrodes are at the same potential. This initial curvature is removed by applying a small voltage difference between the front and back face electrodes. We have tested three DM units and each required slightly different voltage settings to flatten the DM.

PMN is a relaxor ferroelectric material that displays electrostrictive behavior near room temperature [7]. Like piezoelectric materials such as lead zirconium titanate (PZT), electrostrictive materials deform mechanically when an electric field is applied to the material. In contrast to piezoelectrics, in which the direction of deformation reverses with the polarity of the applied field, in electrostriction the deformation direction is independent of the sign of the applied electric field. Although a wide variety of dielectrics possess electrostrictive properties, the effect is particularly large in the relaxor ferroelectrics like PMN. When an electric field is applied to PMN, the material contracts along the transverse axes. In comparison with PZT, PMN has the advantage of greater linearity and lower hysteresis at room temperature.

In the bimorph structure, voltage applied across the top layer generates a tensile stress in the top layer, causing the bimorph to undergo a concave curvature. Similarly, voltage applied across the bottom layer results in convex curvature. In the absence of any residual stress in the two layers, the DM surface is flat whenever an equal voltage is applied across both the top and bottom layers. A mathematical model for the elastic deformation of a bimorph mirror is described in [8]. When a uniform electric field is applied across either the top or bottom ceramic layer, the resulting deflection of the mirror surface is approximately parabolic. Because the front face electrode has a capacitance that is more than 36 times greater than the capacitance of the individual back face electrodes, driving this electrode at high frequencies requires considerably greater power and current from the high voltage drive amplifiers. As a result, when employed in a high bandwidth AO system, the front face electrode is normally biased at a constant 100V, and the mirror is flattened by setting the back face electrodes to approximately 100V (plus or minus a small deviation to correct for residual stress produced during mirror fabrication). Local concave or convex surface deformations are then produced by varying the potential on the individual back face electrodes from 0V to 250V.

Mounting a bimorph DM is a challenging problem, since any constraint at the edges of the DM will reduce the curvature which can be achieved. The AOptix DM is mounted using two rubber o-rings which are preloaded by multiple set-screws arrayed at the outer edge of the mirror [9], as illustrated in Figure 2. The o-ring mount produces translational compliance and near-zero rotational compliance at the DM edge, as described further below.

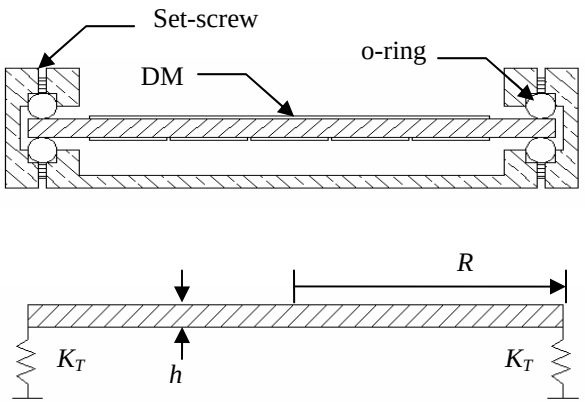

Figure 2: Cross-sectional view of the DM mount (top) and simplified mechanical model for the DM edge supports (bottom).

MODAL RESPONSE MODEL

The free vibration of the DM was analyzed using classical plate theory. Approximating the DM as a thin, uniform, circular plate of PMN, the free vibration of the DM, $w(r, \theta, t)$, is described by the following fourth-order differential equation:

$$(1) \qquad D\nabla^4 w(r,\theta,t) + \rho h \frac{\partial^2 w(r,\theta,t)}{\partial t^2} = 0$$

where $D = Eh^3/\left(12(1-\nu^2)\right)$ denotes the flexural stiffness, and E, ν, ρ, h are the Young's modulus (61 GPa), Poisson's ratio (0.3), density (7.8 g/cc), and thickness of the DM (345 μm). When the plate deflection is decomposed into a spatially varying and a temporally varying component, so that $w(r, \theta, t) = u(r, \theta) \exp(j\omega t)$, the spatial solutions to (1) are mode shapes of the following form:

$$(2) \qquad u_{mn}(r,\theta) = A_{mn}\left[J_m(\beta r) + B_{mn} I_m(\beta r)\right]\cos m\theta$$

where A_{mn} is a normalization constant, B_{mn} is a mode shape parameter, β is an eigenvalue, J_m and I_m denote the m-th order Bessel function of the first kind and the m-th order hyperbolic Bessel function of the first kind, respectively. The eigenvalues of (2) are related to the natural frequencies of the DM by:

$$(3) \qquad f_{mn} = (1/2\pi)(\beta/R)^2 \sqrt{D/(\rho h)}$$

where R is the radius of the DM.

Values for the constants A_{mn}, B_{mn}, and β can be calculated by applying the boundary conditions imposed by the DM mount. These constants were computed using the solution developed by Zagrai and Donskoy for a plate with elastic supports [10]. The translational stiffness of the o-ring support was modeled by first computing the deflection, δ, of the o-ring due to a load per unit length, p, using a Hertzian contact model of a cylinder compressed between two flat surfaces [11]:

$$(4) \qquad \delta(p) = 2pV\left\{1 + \ln\left[\frac{2(2\pi R)^2}{Vpd}\right]\right\}$$

where $V = (1-\nu^2)/(\pi E)$, ν is Poisson's ratio for the rubber o-ring (0.5), E is the Young's modulus for rubber (1.7 MPa), d is the cross-sectional diameter of the o-ring (1 mm), and R is the radius of the o-ring (10 mm). These material constants for the o-ring were estimated based on typical o-ring characteristics and result in reasonable agreement with the experimental data. A linearized compliance per unit length, C_T, was calculated from the slope of the load-deflection model (4) at a given pre-load per unit length, p_0,

$$(5) \qquad C_T = \left.\frac{d\delta(p)}{dp}\right|_{p=p_0} = 2V \ln\left[\frac{2(2\pi R)^2}{Vp_0 d}\right]$$

C_T is relatively insensitive to changes in the pre-load since it has a logarithmic dependence on this parameter. We assumed a pre-load per unit length of 0.16 N/mm. Taking into account the o-rings on both surfaces of the mirror and multiplying the stiffness per unit length by the circumference of the o-rings, the total translational stiffness of the mount was found to be:

$$(6) \qquad K_T = 2\left(2\pi R/C_T\right) = 35 \text{ N/mm}$$

In addition to the flexural natural frequencies described by (3), the DM also has a rigid-body mode due to the DM vibrating in the mirror mount. The natural frequency of this mode is given by:

$$(7) \qquad f_0 = (1/2\pi)\sqrt{K_T/m} = 1.1 \text{ kHz}$$

Where m denotes the mass of the mirror (0.85 g).

EXPERIMENTAL APPARATUS

Dynamic and static measurements of the surface profile of the DM were collected using a stroboscopic phase-shifting interferometer. A block-diagram of the instrument is illustrated in Figure 3. The instrument is a Twyman-Green interferometer in which a piezoelectric stage translates a reference mirror in order to introduce a controlled phase-shift between the light passing through the reference and measurement arms of the interferometer. Surface height variations in the DM create interference fringes when the reference and measurement beams are recombined, producing an interferogram which is captured using a CCD camera. The surface profile of the DM is reconstructed using five interferograms collected at four distinct phase shifts (0, π/2, π, 3π/2) using Hariharan's algorithm [12]. The use of a similar instrument for dynamic characterization of millimeter-sized MEMS devices was first described by Hart, et al. [13]. A previous incarnation of this instrument employed continuous-wave illumination, allowing static surface profiles to be measured [5]. A typical surface profile measurement of the DM obtained using this instrument is displayed in Figure 4. The instrument is capable of measuring the surface profile with an RMS accuracy of approximately 6 nm and an absolute accuracy of ±60 nm across a 10 mm pupil.

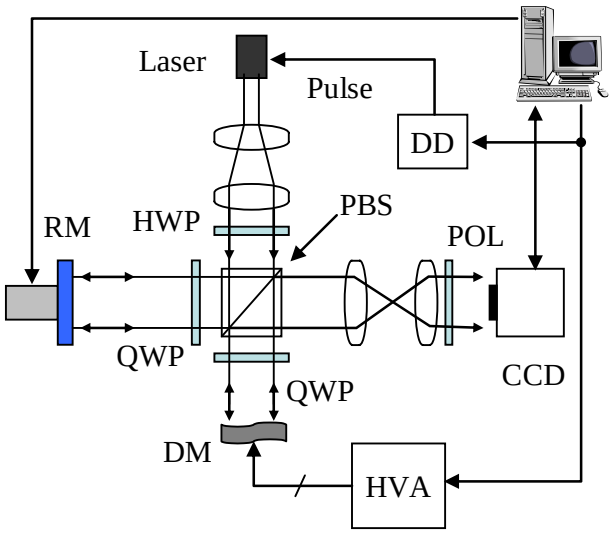

Figure 3: Stroboscopic interferometer block-diagram. RM: Reference Mirror, HWP: Half-wave plate, QWP: Quarter-wave plate, PBS: Polarizing beam-splitter, POL: polarizer, DM: Deformable mirror, HVA: High voltage amplifier, DD: Digital delay.

The interferometer was outfitted with a pulsed diode laser to allow the DM surface profile to be measured in response to time-varying voltage inputs. The 10 mW laser (Hitachi HL6320G) is driven with a custom current source capable of producing optical pulses of less than 1 μsec duration. Strobing the illumination source gates the image, allowing motion at frequencies much faster than the CCD frame rate (30 Hz) to be measured. The strobed illumination is synchronized to the high voltage line used to drive one of the actuators on the DM, and a programmable digital delay unit (Directed Energy model PDG-2510) is used to control the time delay (Δt) between the applied voltage and the optical pulse, as illustrated in Figure 5. By

varying Δt, images of the DM surface at various times throughout the actuation cycle are obtained. Ideally, the optical pulse is sufficiently fast that the DM is essentially motionless during the measurement interval; any motion of the mirror surface during this interval reduces the contrast of the interference fringes and introduces error in the surface measurement. Assuming that the DM undergoes a 1 μm amplitude, 10 kHz sinusoidal oscillation, the maximum motion of the mirror surface over a 1 μsec interval is approximately 63 nm. This is approximately λ/10 for a 635 nm diode laser, representing a small but acceptable reduction in contrast.

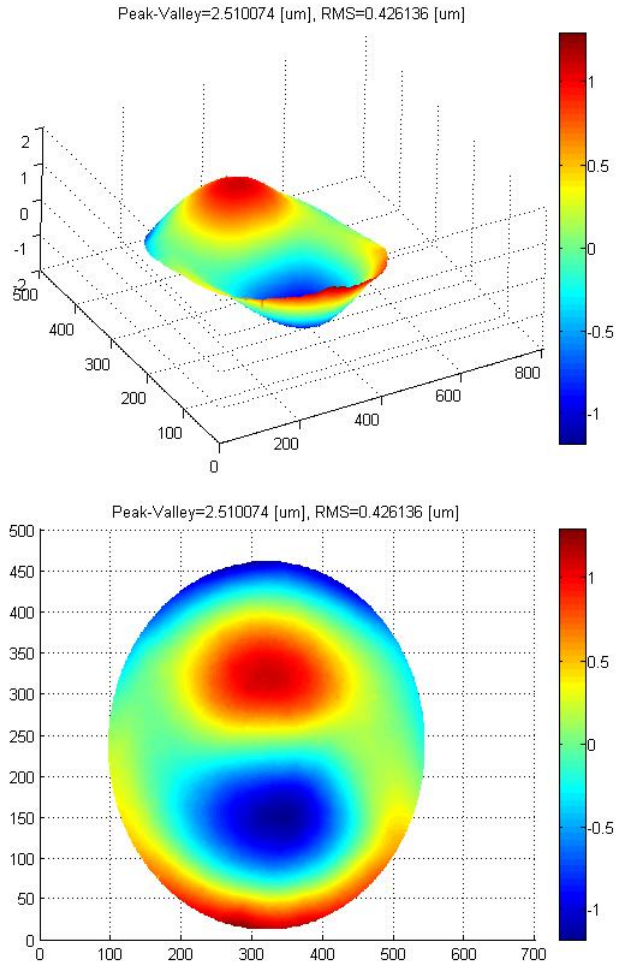

Figure 4: Surface profiles of the DM obtained using the phase-shifting interferometer. The z-height scale is in μm while the x-y axes are measured in CCD pixels.

RESULTS AND DISCUSSION

The dynamic characteristics of two DMs were characterized. These DMs were nearly identical with the exception of a slight difference in the voltages required to flatten the mirror surface. The frequency response of the first DM was first probed using a Laser Doppler Vibrometer (LDV, Polytec OFV-512). Frequency response measurements were obtained using a dynamic signal analyzer (Stanford Research Systems SR780) which was coupled to the front-face electrode of the DM through a high voltage amplifier (Piezo Systems EPA-104-115). The results of this measurement are displayed in Figure 6.

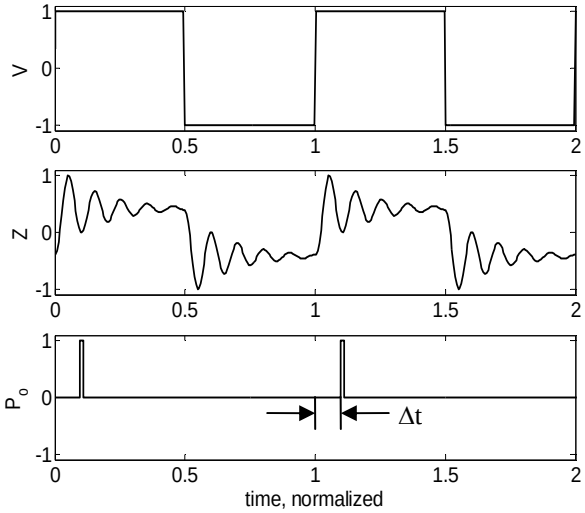

Figure 5: Timing diagram showing applied voltage (V), surface height at a single point on the DM (Z), and optical power from the strobed laser source (P_o).

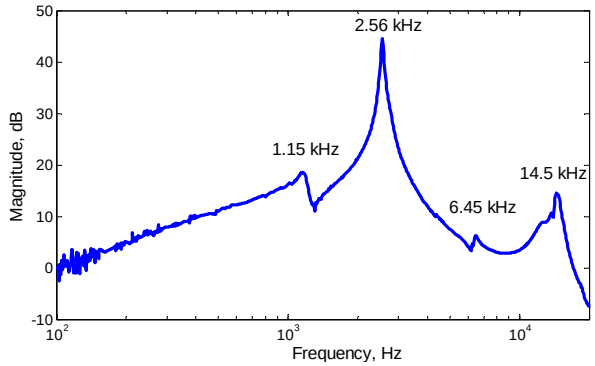

Figure 6: DM frequency response measured with the LDV.

In order to identify the mode shapes associated with each natural frequency, the stroboscopic interferometer was used to record the surface deformation of a second DM in response to step changes in the voltage applied to the back face electrodes. The voltage on all the back face electrodes was initially set to 0V, causing the mirror to assume a parabolic shape. The voltage on the back face electrodes was then set to the voltage required to flatten the DM surface, producing a step disturbance to the mirror. Surface height measurements, $w(r, \theta, t)$, were recorded every 10 μs over a 1 ms interval, for a total of 100 surface measurements. After removing the tilt from each surface, the resulting data set was analyzed by fitting each surface profile measurement with the first four mode shapes defined by (2) using a least-squares fitting algorithm. Mathematically, this can be expressed as:

$$w(r,\theta,t) = \sum_{nm} A_{nm}(t) u_{nm}(r,\theta) + e(r,\theta,t) \quad (8)$$

where nm = 01, 11, 21, 02, and $e(r, \theta, t)$, represents the residual error after the least-squares fit. The frequency content of each mode shape was then identified by computing the FFT of the amplitude coefficients, $A_{mn}(t)$. The magnitude of the FFT of each of these coefficients is displayed in Figure 7. The dominant frequency component of each amplitude coefficient is

summarized in Table 1 along with the natural frequencies measured with the LDV and with the theoretical values predicted from the solution of (3) and (7). The coefficient for the 02 mode shape, A_{02}, appears to contain components from the 01 and 21 modes. We attribute this to the fact that the surface profile measurements obtained with the interferometer only capture the center 10 mm of the DM, making it difficult to entirely resolve the difference between the various mode shapes. In addition, the interferometer is incapable of resolving the rigid-body mode, since the analysis software only accounts for relative difference in the height across the DM, rather than rigid-body translation of the entire DM. The LDV measurements did not capture the 21 mode, suggesting that the LDV measurement beam may have been located on a node for this mode.

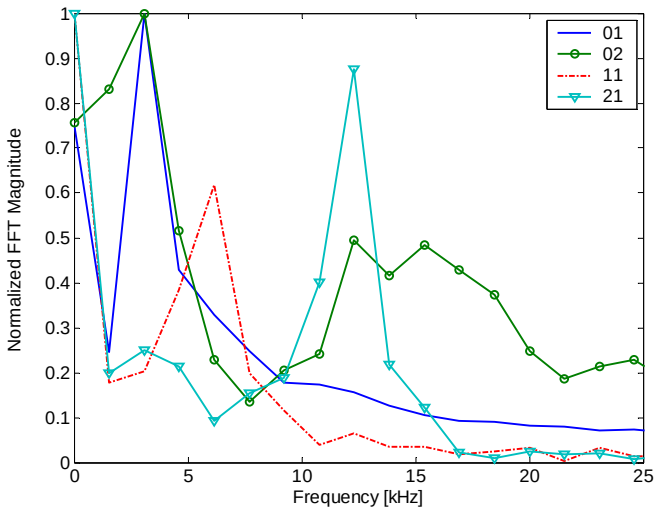

Figure 7: FFT magnitude of measured modal amplitude coefficients.

Table 1: Modal Frequencies

Mode	Model [kHz]	LDV [kHz]	Interferometer [kHz]
Rigid Body	1.1	1.15	-
01	2.8	2.6	3
11	6.7	6.5	6.2
21	11.3	-	12.3
02	13.1	14.5	15.4

CONCLUSIONS

We have reported the measured response of a bimorph DM to transient voltage inputs. The lowest natural frequency of this mirror was measured to be 1.1 kHz, and we attribute this to a rigid-body mode of the DM. Since the DM and wavefront sensors are located at conjugate planes in a typical AO system, the rigid body mode is unlikely to have a measurable impact on the closed-loop performance of the DM. The remaining measured natural frequencies are within 15% of the predictions of a model based on classical plate theory.

ACKNOWLEDGEMENTS

The authors acknowledge the help of Steve Jones from Lawrence Livermore National Laboratories. SPL and JSW are supported by the National Eye Institute (Grant EY 014743).

REFERENCES

[1] G. Vdovin and P. M. Sarro, "Flexible mirror micromachined in silicon," *Applied Optics*, vol. 34, pp. 2968-2972, 1995.

[2] T. Bifano, J. Perrault, R. Mali, and M. Hernstein, "Microelectromechanical Deformable Mirrors," *IEEE Journal of Selected Topics in Quantum Electronics*, vol. 5, pp. 83-89, 1999.

[3] M. A. Helmbrecht, U. Srinivasan, C. Rembe, R. T. Howe, and R. S. Muller, "Micromirrors for Adaptive-Optics Arrays," presented at Transducers 01, 11th Int. Conf. on Solid-State Sensors and Actuators, Munich, Germany, 2001.

[4] Y. Hishinuma, E.-H. Yang, J.-G. Cheng, and S. Trolier-McKinstry, "Optimized design, fabrication and characterization of PZT unimorph microactuators for deformable mirrors," presented at ASME IMECE, Anaheim, CA, 2004.

[5] D. A. Horsley, H. K. Park, S. P. Laut, and J. S. Werner, "Characterization for vision science applications of a bimorph deformable mirror using phase-shifting interferometry," *Proceedings of the SPIE*, vol. 5688, pp. 133-144, 2005.

[6] E. Dalimier and C. Dainty, "Comparative analysis of deformable mirrors for ocular adaptive optics," *Optics Express*, vol. 13, pp. 4275-4285, 2005.

[7] G. H. Haertling, "Ferroelectric ceramics: history and technology," *Journal of the American Ceramic Society*, vol. 82, pp. 797-818, 1999.

[8] E. M. Ellis, "Low-cost bimorph mirrors in adaptive optics", Doctoral Dissertation, Department of Physics, Imperial College of Science Technology and Medicine, 1999

[9] J. E. Graves and M. J. Northcott, "Mounting Apparatus for a Deformable Mirror",U.S. Patent 6,568,647, AOptix Technologies, Inc., 2003

[10] A. Zagrai and D. Donskoy, "A "soft table" for the natural frequencies and modal parameters of uniform circular plates with elastic edge support," *Journal of Sound and Vibration*, vol. 287, pp. 343-351, 2005.

[11] M. J. Puttock and T. E. G. Thwaite, "Elastic compression of spheres and cylinders at point and line contact," Commonwealth Scientific and Industrial Research Organization, National Standards Laboratory Technical Paper, 25, Melbourne, Australia, 1969.

[12] P. Hariharan, B. F. Oreb, and T. Eiju, "Digital Phase-Shifting Interferometry - a Simple Error-Compensating Phase Calculation Algorithm," *Applied Optics*, vol. 26, pp. 2504-2506, 1987.

[13] M. R. Hart, R. A. Conant, K. Y. Lau, and R. S. Muller, "Stroboscopic interferometer system for dynamic MEMS characterization," *Journal of Microelectromechanical Systems*, vol. 9, pp. 409-418, 2000.